Computers in Earth Science Letters (2026) 34-41

Contents lists available at FoundAE

Computers in Earth Science Letters

Journal homepage: https://ejournal.foundae.com/index.php/cesl/index

Resolving near-surface fault architecture in a complex volcanic–sedimentary setting using integrated geophysical methods

Muhammad Amri Aziz Hakim[a,*], Shreeniwas Omanwar[b]

[a] Department of Physics, Institut Teknologi Sumatera, Way Huwi, Jati Agung, South Lampung, Lampung 35365, Indonesia
[b] Department of Physics Near Tapowan, Sant Gadge Baba Amravati University, Maharashtra 444602, India

ARTICLE INFO

Keywords:
Ground penetrating radar
Near-surface faulting
Electrical resistivity imaging
Volcanic–sedimentary environment
Integrated geophysical methods

ABSTRACT

Badung Regency (Bali, Indonesia) is a seismically active region where earthquake events may reactivate local fault systems, posing significant geohazard risks. However, the subsurface fault architecture in this area remains poorly constrained. This study aims to delineate subsurface structures and identify fault zones by integrating Ground Penetrating Radar (GPR) and 2D electrical resistivity imaging using a dipole–dipole configuration. Secondary datasets, including radargrams and geoelectrical measurements, were reprocessed and interpreted using ReflexW 7.0, RES2DINV, and AGI EarthImager. The combined analysis reveals a heterogeneous subsurface composed of clay-rich units (mudstone and silt), alluvium, tuff, breccia, gravel, sand, and limestone. Inverted resistivity values range from 3 to 5116 Ω·m, corresponding to depths of approximately 0.5–50.7 m. Fault zones are inferred from (i) low-resistivity clay layers acting as potential weak zones and (ii) discontinuities and non-hyperbolic reflections observed in GPR profiles. GPR data indicate shallow fault-related features at distances of 280–1100 m along survey lines and depths of 1–8 m. In contrast, resistivity imaging identifies deeper structural discontinuities at distances of 47–196 m and depths of 0.6–39.3 m. The discrepancy in detected depths highlights the complementary sensitivity of both methods to different structural scales. These results demonstrate that integrating GPR and electrical resistivity imaging provides a robust approach for resolving near-surface fault geometry in complex volcanic–sedimentary environments. The identified fault zones may represent reactivated structures associated with regional seismicity, underscoring their importance for local hazard assessment and land-use planning.

1. Introduction

Near-surface fault systems play a critical role in controlling geological hazards, groundwater flow, and subsurface fluid migration, particularly in tectonically and volcanically active regions. In areas characterized by complex volcanic–sedimentary settings, such as Bali, Indonesia, the identification and characterization of shallow fault structures remain challenging due to lithological heterogeneity, rapid facies changes, and strong weathering processes. These conditions often obscure structural signatures at the surface, making subsurface geophysical investigations essential for resolving fault architecture and assessing associated risks [1, 2].

Indonesia is located within one of the most tectonically active regions in the world, influenced by the convergence of the Indo-Australian, Eurasian, and Pacific plates. This tectonic framework results in frequent seismic activity and widespread fault development, including both regional and local fault systems. Bali, as part of the Sunda Arc, is particularly influenced by subduction-related processes and volcanic activity [3–5]. Previous studies have highlighted the presence of active faults and seismic hazards across the island; however, the detailed geometry and distribution of near-surface faults in specific regions, such as Badung Regency, remain poorly constrained. This lack of detailed structural information poses challenges for hazard mitigation, infrastructure planning, and sustainable land use [6, 7].

Badung Regency is a rapidly developing area in Bali, characterized by dense population, tourism infrastructure, and ongoing urban expansion (Fig. 1). The occurrence of past earthquake events in this region raises concerns about the potential reactivation of local fault systems. Shallow faults, even with small displacements, can significantly impact ground stability and pose risks to buildings, roads, and other critical infrastructure. Therefore, a detailed understanding of near-surface fault architecture is essential for improving local geohazard assessments [8–10].

* Corresponding author.
E-mail address: muhammadhakim@gmail.com (M. A. A. Hakim).

https://doi.org/10.58524/cesl.v1i1.126
Received 17 January 2026; Received in revised form 10 February 2026; Accepted 20 February 2026
Available online 1 March 2026
XXXX-XXXX/Published by FoundAE (Foundation of Advanced Education).

Conventional geological mapping techniques are often insufficient for detecting shallow subsurface structures in such environments, particularly where surface expressions of faults are subtle or absent. As a result, near-surface geophysical methods have become indispensable tools for imaging subsurface structures. Among these, Ground Penetrating Radar (GPR) and electrical resistivity imaging (ERI) are widely used due to their complementary capabilities. GPR is highly effective for high-resolution imaging of shallow subsurface features, particularly in detecting discontinuities, fractures, and stratigraphic boundaries. It provides detailed information on subsurface reflectivity patterns, allowing the identification of anomalies such as hyperbolic reflections and signal discontinuities associated with structural features [3, 11].

On the other hand, electrical resistivity imaging offers insights into the subsurface distribution of electrical properties, which are closely related to lithology, porosity, fluid content, and degree of weathering. The dipole–dipole array configuration is particularly sensitive to lateral resistivity variations, making it suitable for detecting fault zones and structural discontinuities. Fault zones often exhibit distinct resistivity contrasts due to fracturing, fluid accumulation, or the presence of clay-rich materials, which act as zones of weakness. By combining GPR and resistivity methods, it is possible to overcome the limitations of each individual technique and achieve a more robust interpretation of subsurface structures [12, 13].

Despite the widespread use of these methods, studies integrating GPR and resistivity imaging in tropical volcanic–sedimentary environments remain relatively limited. The complexity of such settings, including high moisture content, conductive clay layers, and heterogeneous lithology, can significantly affect data quality and interpretation. Therefore, there is a need for case studies that demonstrate the effectiveness of integrated geophysical approaches in resolving near-surface fault architecture under these challenging conditions [6, 14, 15].

This study aims to delineate near-surface fault structures in Badung Regency, Bali, by integrating GPR and 2D electrical resistivity imaging data. Specifically, the objectives are to (1) characterize the subsurface lithological framework, (2) identify structural discontinuities associated with fault zones, and (3) evaluate the effectiveness of combining GPR and resistivity methods in a complex volcanic–sedimentary environment. Secondary datasets, including radargrams and geoelectrical measurements, are reprocessed and analyzed using advanced software tools to enhance data quality and interpretation reliability [4, 16].

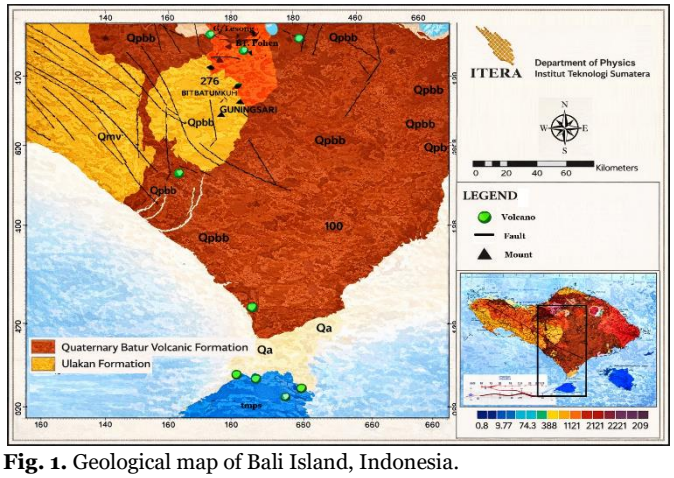

Fig. 1. Geological map of Bali Island, Indonesia.

The integration of these datasets allows for a multi-scale analysis of subsurface structures. GPR provides high-resolution imaging of shallow features, typically within the upper few meters, while resistivity imaging extends the investigation depth and captures broader structural trends. The complementary nature of these methods enables the identification of both shallow and relatively deeper fault-related features, providing a more comprehensive understanding of fault geometry [17, 18].

The significance of this study lies in its contribution to both methodological development and regional geohazard assessment. From a methodological perspective, it demonstrates the advantages of integrating multiple geophysical techniques to address the challenges posed by complex geological environments. From an applied perspective, the results provide valuable insights into the distribution and characteristics of near-surface faults in Badung Regency, which can inform hazard mitigation strategies and land-use planning [19–21].

Furthermore, this study contributes to the broader understanding of fault development in volcanic–sedimentary systems, where interactions between tectonic, volcanic, and sedimentary processes create highly heterogeneous subsurface conditions. The findings may also be relevant to other regions with similar geological settings, particularly in Southeast Asia and other parts of the Pacific Ring of Fire [3, 6, 16].

In conclusion, resolving near-surface fault architecture in complex geological environments requires an integrated approach that combines high-resolution imaging with reliable subsurface property characterization. By applying GPR and electrical resistivity imaging in Badung Regency, this study provides new insights into shallow fault systems and highlights the importance of multi-method geophysical investigations for improving our understanding of subsurface structures and associated geohazards [3, 11].

1.1. Geological setting of the study area

Bali Island is located between Java and Lombok Islands, within the Lesser Sunda Islands of Indonesia, at coordinates 8°3′38″–8°50′56″ S and 114°25′53″–115°42′39″ E, covering an area of approximately 5,636.66 km². Administratively, Badung Regency is situated in the southern part of Bali Province and encompasses several districts, including Kuta, Abiansemal, Mengwi, and Petang. The study area is characterized by rapid urban development, particularly in coastal zones, which increases its vulnerability to geological hazards [6, 14, 15].

The regional geology of Badung Regency is strongly influenced by volcanic activity associated with several volcanic complexes, including the Batukaru Volcano, the Lesong–Poheng–Sengayang volcanic group, the ancient Buyan–Bratan volcanic complex, and the younger Buyan–Bratan and Batur volcanic systems. These volcanic centers have contributed significantly to the lithological diversity of the region, resulting in a complex volcanic–sedimentary sequence [4, 16].

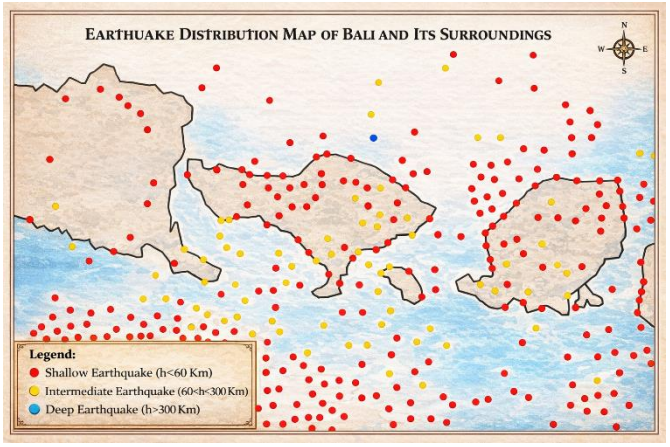

Fig. 2. The spatial distribution of earthquake occurrences around Bali.

The Batukaru volcanic system primarily produces pyroclastic deposits such as sandy tuff, volcanic breccia, and lahar deposits. In contrast, the coastal areas of Kuta are dominated by alluvial and marine deposits, consisting mainly of unconsolidated sands derived from coastal processes. The southern part of Badung Regency is characterized by carbonate hills composed of marl (clay-rich limestone containing aragonite), calcareous sandstone, and limestone, indicating a transition from volcanic to sedimentary depositional environments [17, 18].

In addition, volcanic products from the Lesong–Poheng–Sengayang, ancient Buyan–Bratan, and Batur volcanic systems have contributed intermediate volcanic deposits, including volcanic ash, tuff, breccia, lahar, gravel, and sand. This combination of volcanic and sedimentary processes results in highly heterogeneous subsurface conditions, which complicate geological interpretation and structural analysis [6, 14, 15].

Tectonically, Bali Island forms part of the Sunda volcanic arc, which developed as a result of the subduction of the Indo-Australian Plate beneath the Eurasian Plate. This convergent tectonic setting generates intense seismic activity and plays a key role in shaping the geological structure of the region. The tectonic framework of Bali is controlled by two major seismic sources: (1) the subduction zone located (south) of the island and (2) the Flores back-arc thrust system located to the north. The interaction between these tectonic features creates a complex stress regime, which contributes to both deep and shallow seismicity. Morphologically, Bali exhibits a basin-like structure, particularly in its northern part, which is interpreted as a result of tectonic deformation associated with back-arc thrusting. This structural configuration reflects the dynamic interaction between compressional forces from subduction and extensional or transpressional processes within the arc system.

The primary driver of seismic activity in Bali is the ongoing convergence between the Indo-Australian Plate and the Eurasian Plate along the Sunda subduction zone. This tectonic interaction extends from Romang Island in the east to the Sunda Strait in the west and generates numerous earthquake sources along the Java subduction zone. Earthquakes in the Bali region are generally classified into three categories based on depth: shallow, intermediate, and deep earthquakes. In southern Bali, seismic activity is commonly associated with intermediate-depth earthquakes (approximately 150–200 km), which are linked to subduction processes. However, shallow earthquakes also occur, particularly in the northern Bali basin, and are often associated with local fault systems and back-arc thrust activity.

Seismicity data from the Meteorological, Climatological, and Geophysical Agency (BMKG) indicate that earthquake activity in the Bali region is spatially distributed across a wide area, including regions (west) of Sumbawa and Sumba Islands. The seismicity pattern suggests the presence of active tectonic structures that may influence local geological conditions, including the reactivation of near-surface faults in areas such as Badung Regency.

2. Method

2.1. Study area and data acquisition

This study was conducted in Badung Regency, Bali Province, Indonesia, between January and February 2021. The study area represents a complex volcanic–sedimentary environment influenced by active tectonics and rapid urban development, making it suitable for investigating near-surface fault structures.

This study utilizes secondary geophysical datasets obtained from the Geological Survey Center, Ministry of Energy and Mineral Resources (Indonesia) [6, 14, 15]. The datasets consist of:

- Ground Penetrating Radar (GPR) radargrams
- Electrical resistivity data acquired using a dipole–dipole configuration

These datasets were selected due to their high resolution and relevance for imaging shallow subsurface structures. Subsequent processing and interpretation were carried out to identify subsurface lithology and fault-related features in the study area.

2.2. Geophysical methods

2.2.1. Ground penetrating radar (GPR)

GPR is a high-resolution geophysical method that utilizes electromagnetic wave propagation to image shallow subsurface structures (Fig. 3). In this study, GPR data were acquired using a GSSI SIR-20 system equipped with a 200 MHz antenna, which provides a balance between penetration depth and resolution. The method is particularly effective for detecting shallow discontinuities such as fractures, faults, and stratigraphic boundaries. Variations in dielectric properties of subsurface materials generate reflected signals recorded as radargrams. Structural features, including faults, are interpreted from reflection patterns such as signal discontinuities, chaotic zones, and non-hyperbolic anomalies [14, 22, 23].

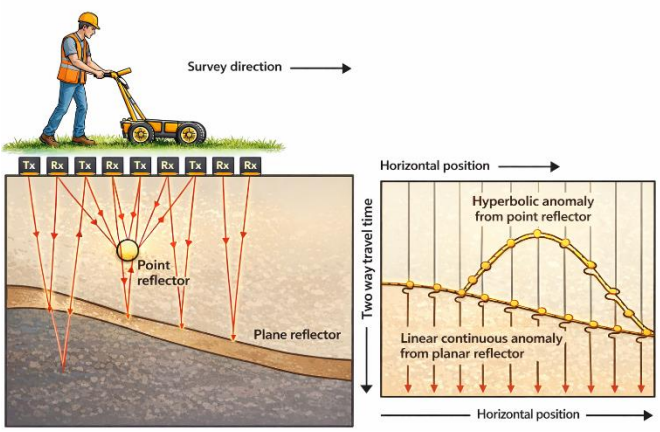

Fig. 3. The ground-penetrating radar (GPR) method.

The effectiveness of GPR surveys strongly depends on survey design, which includes defining clear objectives and understanding the subsurface conditions of the study area. These factors are critical for optimizing data acquisition and ensuring reliable interpretation. One of the key parameters in GPR surveys is the antenna frequency, which controls both the depth of penetration and the spatial resolution of the data. Lower-frequency antennas allow deeper signal penetration but with reduced resolution, whereas higher-frequency antennas provide higher resolution but are limited to shallower depths. Therefore, the selection of antenna frequency must be carefully adjusted according to the depth and size of the target [17, 18].

In addition, survey line configuration plays an important role in accurately imaging subsurface features. GPR profiles are typically arranged parallel or perpendicular to the expected orientation of geological structures to maximize detection capability. The spacing between survey lines is determined by the scale of the target; closely spaced lines are required to resolve small or complex features, while wider spacing may be sufficient for larger structures [6, 14, 15].

The interpretation of GPR data is based on the analysis of reflected electromagnetic signals recorded as radargrams. Subsurface features are identified through characteristic reflection patterns, including hyperbolic signatures, signal discontinuities, amplitude variations, and zones of attenuation. In particular, fault zones are commonly recognized by disrupted or offset reflectors, chaotic reflection patterns, and changes in signal continuity.

Overall, GPR provides a powerful, non-invasive tool for high-resolution imaging of shallow subsurface structures. However, its performance may be limited in conductive environments, such as clay-rich or water-saturated materials, which can attenuate electromagnetic signals and reduce penetration depth. Therefore, GPR is often integrated with other geophysical methods to improve interpretation reliability [1, 2].

2.3. Electrical resistivity imaging (ERI)

Electrical resistivity imaging (ERI) was applied using a multi-channel SuperSting R8 system with a dipole–dipole array configuration (Fig. 4). This array is highly sensitive to lateral resistivity variations, making it suitable for detecting structural discontinuities such as fault zones. The method measures apparent resistivity, which reflects subsurface variations in lithology, porosity, fluid content, and degree of weathering. Fault zones are typically associated with resistivity contrasts due to fracturing, clay accumulation, or fluid pathways [14, 22, 23].

The electrical resistivity method is a geophysical technique that characterizes subsurface materials based on their electrical properties, particularly resistivity, which is controlled by lithology, porosity, fluid content, and degree of weathering. This method is widely used to investigate subsurface geological structures, including stratigraphy, fracture zones, and faults. Geoelectrical methods can be broadly classified into passive and active approaches [6, 14, 15].

Passive methods rely on naturally occurring electrical fields, whereas active methods involve the injection of artificial current into the ground. Electrical resistivity imaging (ERI), applied in this study, is an active method in which electrical current is introduced into the subsurface through current electrodes, and the resulting potential differences are measured using potential electrodes. These measurements are then used to calculate apparent resistivity, which is subsequently inverted to obtain the true resistivity distribution of subsurface materials [8].

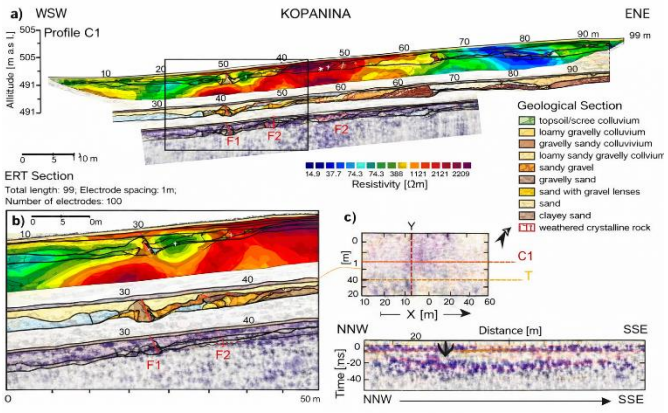

Fig. 4. Identify the signs of fault presence using two methods: the ground-penetrating radar method and the electrical resistivity method.

The resistivity method offers several advantages, including its non-destructive nature, relatively low operational cost, and efficiency in data acquisition compared to invasive techniques such as drilling. Moreover, it provides continuous two-dimensional (2D) or three-dimensional (3D) subsurface models, which are essential for identifying lateral and vertical variations in geological structures. Fault zones can be effectively detected using resistivity methods due to the presence of electrical contrasts associated with fracturing, fluid accumulation, and clay-rich materials [6, 14, 15].

These zones often appear as low-resistivity anomalies or sharp resistivity discontinuities in inverted models. However, interpretation of resistivity data is inherently non-unique, meaning that similar resistivity values may correspond to different lithological conditions. Therefore, integration with other geophysical methods, such as Ground Penetrating Radar (GPR), is necessary to improve interpretation reliability.

Previous studies have demonstrated the effectiveness of combining resistivity and GPR methods for fault detection. For example, Fischer et al. (2012) identified fault-related discontinuities at depths of approximately 10–20 m using GPR, which were further corroborated by resistivity imaging at greater depths (40–60 m). This multi-method approach highlights the complementary strengths of geophysical techniques in resolving both shallow and deeper structural features, thereby providing a more comprehensive understanding of subsurface fault systems [6, 14, 15].

2.4. Data integration and interpretation

Interpretation was conducted through an integrated analysis of GPR and resistivity datasets to improve reliability and reduce ambiguity. GPR data were interpreted both qualitatively and quantitatively. Qualitative interpretation focuses on identifying reflection patterns such as:

- Discontinuities in stratigraphic layers
- Chaotic or disrupted reflection zones
- Anomalous signal attenuation

Quantitative interpretation involves estimating depths and geometries of subsurface features based on signal travel time and wave velocity assumptions.

- Resistivity data interpretation was based on:
- Resistivity contrasts between lithological units
- Identification of low-resistivity zones (e.g., clay-rich or fractured zones)
- Detection of structural discontinuities

These features were correlated with geological information to identify potential fault zones.

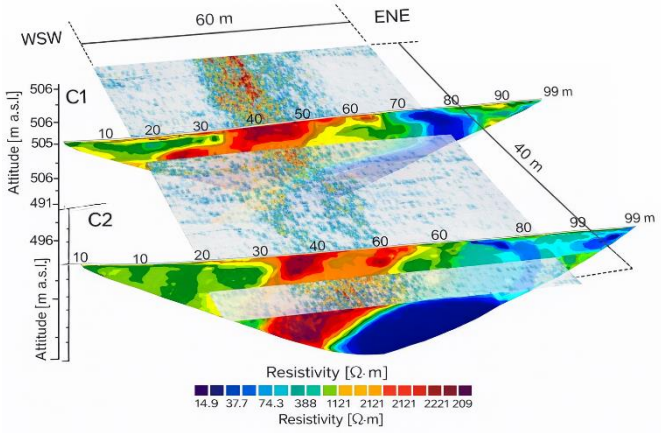

Fig. 5. Integration of two methods for detecting the presence of faults.

The integration of GPR and resistivity results allows for a multi-scale characterization of subsurface structures (Fig.5). GPR provides high-resolution imaging of shallow features, while resistivity data extend the investigation depth and highlight broader structural trends.

- Fault zones were identified based on the following combined criteria:
- Coincidence of GPR reflection discontinuities and resistivity contrasts
- Presence of low-resistivity zones associated with weak or fractured materials
- Consistent structural alignment across multiple survey lines.

3. Results and discussion

3.1. Identification of fault structures in Jimbaran village, South Kuta district, Badung regency

Data processing along the first survey line was conducted in Jimbaran Village, South Kuta District, Badung Regency. The analysis produced two main subsurface representations: a two-dimensional radargram derived from Ground Penetrating Radar (GPR) data (Fig. 6) and a resistivity cross-section obtained from the electrical resistivity method (Fig. 7). These complementary geophysical methods enable a more robust interpretation of subsurface structures.

The resistivity section indicates that zones with resistivity values ranging from 3 to 78.7 Ω·m, at depths between 0.51 and 3.80 m, correspond to lithological units such as shale, dolomite, and limestone. Meanwhile, higher resistivity values ranging from 224 to 5116 Ω·m, observed at depths of 5 to 31.7 m, are interpreted as clay-rich materials (including mudstone and silt), alluvial

deposits, gravel, and sand. This variation reflects heterogeneity in lithology and sediment composition within the study area.

A distinct anomaly is observed in the resistivity profile at a horizontal distance of 56–72 m and a depth of 8–11 m, characterized by a resistivity value of approximately 635 Ω·m. This anomaly is interpreted as a fault zone within a clay-dominated layer, likely representing a structural discontinuity that disrupts the surrounding stratigraphy. Furthermore, the radargram section reveals a fractured zone at a measurement distance of approximately 1000–1100 m and at shallow depths of 0–4.5 m. This zone is characterized by non-hyperbolic anomalies forming discontinuous planar features, which are indicative of fault planes or structural discontinuities. Such features are commonly associated with fault-related deformation and fracture systems.

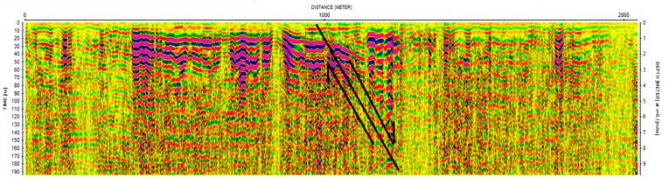

Fig. 6. Radargram cross-section indicating fault structures in Pelaga Village, Petang Sub-district, Badung Regency.

The integration of resistivity and GPR data strengthens the interpretation that the identified anomalies represent fault structures. The presence of clay layers combined with non-hyperbolic discontinuities in the radargram is consistent with previous studies identifying fault zones using similar geophysical signatures. Therefore, the study area is strongly inferred to contain fault structures, which may have implications for local geohazards and land-use planning.

Based on the combined interpretation of the GPR radargram and resistivity cross-section, it can be concluded that a fault structure is present in Jimbaran Village, South Kuta District, Badung Regency. The identified structure is interpreted as a reverse fault, as indicated by a dip angle of approximately 35°, which is less than 45°, and by the relative displacement pattern where the footwall block appears to have subsided relative to the hanging wall block. This structural configuration is consistent with compressional tectonic settings and aligns with previously reported fault characteristics in similar geological environments.

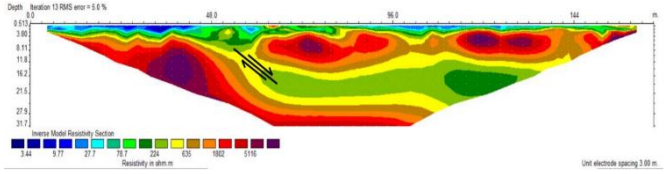

Fig. 7. Resistivity cross-section indicating a fault structure in Jimbaran Village, South Kuta Sub-district, Badung Regency.

3.2. *Identification of fault structures in Pelaga village, Petang district, Badung regency*

Data processing along the second survey line was conducted in Pelaga Village, Petang District, Badung Regency. The analysis produced two primary subsurface images: a radargram derived from Ground Penetrating Radar (GPR) data (Fig. 8) and a resistivity cross-section obtained from the electrical resistivity method (Fig. 9). The integration of these methods provides complementary information for identifying subsurface structural features. The resistivity section indicates that zones with resistivity values ranging from 734 to 1807 Ω·m, at depths between 0.62 and 6.12 m, are interpreted as layers composed of tuff, gravel, and sand. In contrast, zones with lower resistivity values ranging from 8.12 to 298 Ω·m, observed at depths of 8 to 42.9 m, correspond to marl, clay, and argillaceous materials. These variations reflect differences in lithological composition and moisture content within the subsurface.

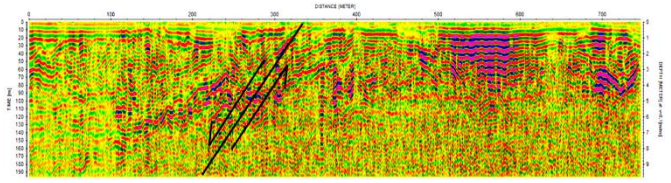

Fig. 8. Radargram cross-section indicating fault structures in Pelaga village, Petang Sub-district, Badung regency.

A significant anomaly is identified in the resistivity profile at a horizontal distance of 47–53 m and at depths of 8–25 m, characterized by resistivity values between 8.12 and 298 Ω·m. This anomaly represents a discontinuity zone within clay-rich material, which is interpreted as a fault plane or structural discontinuity disrupting the surrounding geological layers [24].

The radargram section further supports this interpretation by revealing a fractured zone at a measurement distance of approximately 280–320 m and at depths of 3–6 m. This zone is characterized by non-hyperbolic reflection patterns forming planar discontinuities, which are commonly associated with fault structures and fracture zones. The consistency between the resistivity anomalies and the radargram features strengthens the interpretation that a fault structure exists in the study area. The presence of clay-rich layers combined with non-hyperbolic discontinuities in the GPR data is widely recognized as a reliable indicator of fault zones in near-surface geophysical investigations. Therefore, the identified anomalies are strongly interpreted as representing a fault structure in Pelaga Village, which may have important implications for geological hazards and subsurface stability in the region.

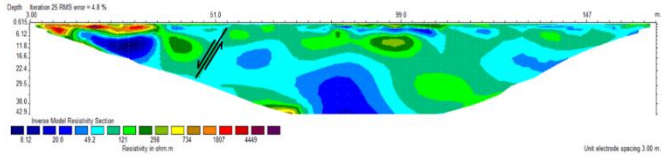

Fig. 9. Resistivity cross-section indicating the presence of a fault structure in Pelaga village, Petang Sub-district, Badung regency.

3.3. *Identification of fault structures in Mengwi district, Badung regency*

Data processing along the third survey line was conducted in Mengwi District, Badung Regency. The analysis produced two primary subsurface representations: a radargram derived from Ground Penetrating Radar (GPR) data (Fig. 10) and a resistivity cross-section obtained from the electrical resistivity method (Fig. 11). The integration of these two geophysical methods enhances the reliability of subsurface structural interpretation.

The resistivity section indicates that zones with resistivity values ranging from 3.93 to 14 Ω·m, at depths between 0.82 and 9 m, are interpreted as sandy tuff layers. In contrast, zones with higher resistivity values ranging from 26.4 to 336 Ω·m, observed at depths of 10.5 to 50.7 m, correspond to silty clay, gravel, and sand deposits. These variations reflect differences in lithology, grain size, and water content within the subsurface.

A distinct anomaly is identified in the resistivity profile at a horizontal distance of 138–144 m and at depths of 10.5–39.3 m, characterized by resistivity values between 26.4 and 336 Ω·m. This anomaly represents a discontinuity within a silty clay layer, which is interpreted as a fault zone that disrupts the continuity of subsurface strata.

The radargram section further supports this interpretation by revealing a fractured zone at a measurement distance of approximately 1020–1080 m and at shallow depths of 1.5–4 m. This zone is characterized by non-hyperbolic reflection patterns forming planar discontinuities, which are indicative of fault planes or fracture zones. Such features are commonly associated with structural deformation in near-surface geophysical investigations.

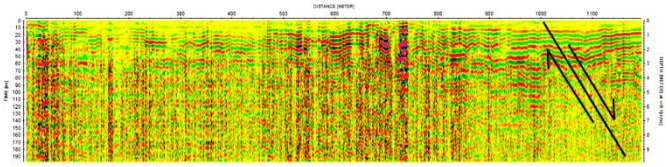

Fig. 10. Radargram cross-section indicating fault structures in Mengwi Sub-district, Badung regency.

The consistency between anomalies observed in both resistivity and GPR data strongly suggests the presence of a fault structure in the Mengwi District. The occurrence of clay-rich layers combined with non-hyperbolic discontinuities in the radargram is widely recognized as a diagnostic indicator of fault zones in previous studies.

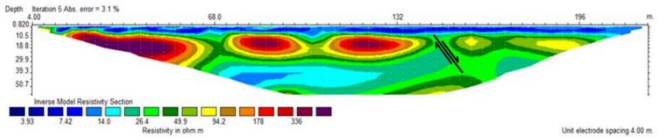

Fig. 11. Resistivity cross-section indicating fault structures in Mengwi Sub-district, Badung regency.

Based on the integrated interpretation of both methods, the identified structure is classified as a normal fault. This interpretation is supported by a dip angle of approximately 55°, which is relatively steep and approaches vertical geometry, as well as by the displacement pattern in which the hanging wall block has moved downward relative to the footwall block. This structural configuration is characteristic of extensional tectonic regimes and indicates that the study area may be influenced by local extensional stress conditions.

The identification of this fault structure has important implications for subsurface stability, groundwater flow pathways, and potential geohazards in the Mengwi District. Furthermore, the results demonstrate the effectiveness of integrating GPR and resistivity methods for detecting and characterizing shallow subsurface fault systems.

3.4. *Identification of fault structures in Banjar Wijaya Kusuma, Ungasan village, South Kuta district, Badung regency*

Data processing along the fourth survey line was conducted in Banjar Wijaya Kusuma, Ungasan Village, South Kuta District, Badung Regency. The analysis produced two main subsurface representations: a radargram derived from Ground Penetrating Radar (GPR) data (Fig. 12) and a resistivity cross-section obtained from the electrical resistivity method (Fig. 13). The integration of these two geophysical approaches enables a more comprehensive interpretation of subsurface structures.

The resistivity section indicates that zones with resistivity values of approximately 736 Ω·m, at depths between 0.68 and 10.8 m, are interpreted as alluvial deposits and clay layers. Meanwhile, zones with higher resistivity values ranging from 198 to 3834 Ω·m, observed at depths of 12 to 42.2 m, correspond to more consolidated lithologies such as limestone, carbonate rocks, and breccia. These variations reflect differences in lithology, porosity, and degree of consolidation within the subsurface. A distinct anomaly is observed in the resistivity profile at a horizontal distance of 180–196 m and at shallow depths of 0.68–10.8 m, characterized by resistivity values around 736 Ω·m. This anomaly represents a discontinuity within a clay-dominated layer, which is interpreted as a fault zone disrupting the continuity of the surrounding strata.

The radargram section further supports this interpretation by revealing a fractured zone at a measurement distance of approximately 480–580 m and at depths of 5–8 m. This zone is characterized by non-hyperbolic reflection patterns forming two distinct planar discontinuities, which are indicative of fault planes. Such non-hyperbolic anomalies are commonly associated with structural discontinuities and fracture systems in near-surface geophysical investigations [20, 21, 25].

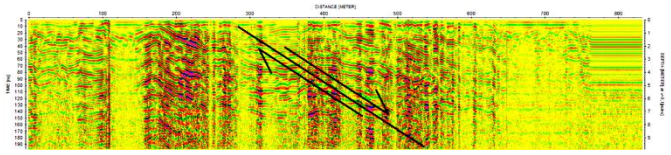

Fig. 12. Radargram cross-section indicating the fault structure at Banjar Wijaya Kusuma, Ungasan village, South Kuta district, Badung regency.

The consistency between anomalies observed in both the resistivity and GPR data provides strong evidence for the presence of a fault structure in the study area. The occurrence of clay-rich layers combined with non-hyperbolic planar reflections is widely recognized as a reliable indicator of fault zones. Therefore, the integrated geophysical interpretation confirms the existence of a fault structure in Banjar Wijaya Kusuma, Ungasan Village, which may have important implications for subsurface stability, groundwater pathways, and local geohazard assessment [16, 26, 27].

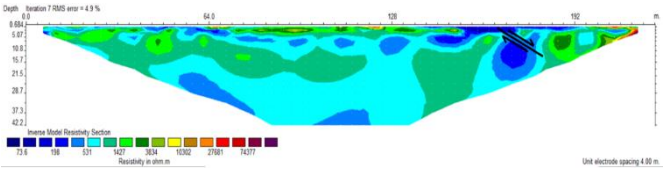

Fig. 13. Resistivity cross-sections indicating fault structures in Banjar Wijaya Kusuma, Ungasan village, South Kuta district, Badung regency.

3.5. *Identification of fault structures in Garuda Wisnu Kencana, Ungasan village, South Kuta district, Badung regency*

Data processing along the fifth survey line was conducted in the Garuda Wisnu Kencana area, Ungasan Village, South Kuta District, Badung Regency. The analysis produced two two-dimensional subsurface models: a radargram derived from Ground Penetrating Radar (GPR) data (Fig. 14) and a resistivity cross-section obtained using the electrical resistivity method with a dipole–dipole configuration (Fig. 15). The integration of these methods provides complementary insights into the subsurface structure and enhances the reliability of interpretation.

The resistivity section indicates that zones with high resistivity values ranging from 4381 to 14,363 Ω·m, at depths between 0.68 and 10.8 m, are interpreted as alluvial deposits, clay, and sandy tuff. Meanwhile, zones with resistivity values of approximately 1057 Ω·m, observed at depths of 11 to 42.2 m, correspond to limestone, gravel, and sand layers. These variations reflect differences in lithological composition, porosity, and consolidation within the subsurface [28, 29].

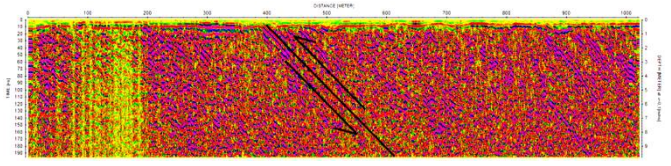

Fig. 14. Radar cross-section indicating fault structures at Garuda Wisnu Kencana, Ungasan Village, South Kuta district, Badung regency.

A distinct discontinuity anomaly is observed in the resistivity profile at a horizontal distance of 188–192 m and at shallow depths of 0.68–10.8 m, characterized by resistivity values ranging from 4381 to 14,363 Ω·m. This anomaly is interpreted as a fault-related discontinuity within a clay-dominated layer, indicating structural deformation that disrupts the continuity of subsurface strata.

The radargram section further supports this interpretation by revealing a fractured zone at a measurement distance of approximately 400–500 m and at shallow depths of 1–4 m. This zone is characterized by non-hyperbolic reflection patterns forming planar discontinuities, which are indicative of fault planes. Such anomalies are widely recognized as diagnostic features of fault structures in near-surface geophysical investigations.

The consistency between anomalies observed in both resistivity and GPR data provides strong evidence for the presence of a fault structure in the study area. The occurrence of clay-rich layers combined with non-hyperbolic discontinuities reinforces the interpretation of a structurally controlled zone, which is consistent with previous findings in similar geological settings.

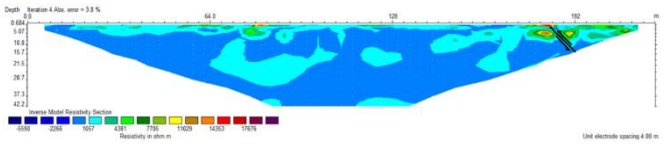

Fig. 15. Resistivity cross-sections indicating fault structures in Garuda Wisnu Kencana, Ungasan Village, South Kuta district, Badung regency.

Based on the integrated interpretation, the identified structure is classified as a reverse fault, characterized by a dip angle of approximately 45°. This interpretation is supported by the displacement pattern in which the hanging wall block has moved upward relative to the footwall block, indicating compressional tectonic conditions. This structural configuration suggests that the study area has been influenced by compressional stress regimes, which may have implications for subsurface stability, groundwater flow, and geohazard potential

3.6. Geological interpretation

The geological evolution of Bali Island is closely related to marine and volcanic processes that have occurred since the Early Miocene. During this period, submarine volcanic activity produced pillow lava and volcanic breccia interbedded with limestone deposits. In southern Bali, carbonate sedimentation dominated, forming the Southern Formation. In contrast, northern Bali experienced the deposition of finer-grained sediments and organic materials during the Pliocene, resulting in the Asah Formation. Subsequent volcanic activity during the Pliocene further contributed to the development of several geological formations across Bali, including the Ulakan, Prapatagung, Jembrana, and Palasari Formations, as well as volcanic complexes such as Buyan–Bratan–Batur and Mount Agung.

The integrated interpretation of two-dimensional (2D) resistivity and GPR data across the five survey lines reveals significant lateral and vertical heterogeneity in subsurface lithology. Variations in resistivity values reflect differences in lithological composition, grain size, porosity, and water content. In general, lower resistivity values (e.g., <100 Ω·m) are associated with clay-rich and fine-grained sediments, while higher resistivity values (>1000 Ω·m) indicate more consolidated materials such as limestone, breccia, and coarse-grained deposits.

Across all survey lines, the resistivity models consistently identify two main subsurface units: (1) shallow layers dominated by unconsolidated or semi-consolidated materials such as alluvium, clay, sandy tuff, and fine sediments, and (2) deeper layers consisting of more consolidated lithologies such as limestone, marl, breccia, and coarse clastic deposits. This stratigraphic pattern reflects the transition from surface depositional environments to more compacted geological formations at depth.

The GPR radargrams provide complementary information by highlighting structural discontinuities and fracture zones in the shallow subsurface. Across all survey lines, zones characterized by non-hyperbolic reflection patterns and planar discontinuities are consistently identified at shallow depths (generally <10 m). These features are interpreted as fracture zones or fault planes, which disrupt the continuity of subsurface reflectors.

The integration of resistivity and GPR data clearly indicates the presence of fault structures along all five survey lines. Fault zones are characterized by (1) resistivity anomalies associated with clay-rich or disturbed materials, (2) discontinuities in subsurface layering, and (3) non-hyperbolic planar reflections in radargrams. These characteristics are widely recognized as diagnostic indicators of fault zones in near-surface geophysical investigations.

The identified fault structures exhibit varying kinematic characteristics, including normal faults and reverse faults. Normal faults are characterized by the downward movement of the hanging wall relative to the footwall, typically associated with extensional stress regimes. In contrast, reverse faults are characterized by the upward movement of the hanging wall, indicating compressional tectonic forces. The coexistence of these fault types suggests a complex tectonic regime in the study area, potentially influenced by both local stress redistribution and regional tectonic interactions.

From a regional perspective, Bali is located within an active tectonic setting influenced by the subduction of the Indo-Australian Plate beneath the Eurasian Plate. This tectonic environment generates significant compressional forces, volcanic activity, and structural deformation. However, local geological conditions, including lithological heterogeneity and volcanic processes, may also contribute to the development of extensional structures at shallow depths.

Seismic activity in Badung Regency further supports the presence of active tectonic processes in the region. According to data from the Ministry of Energy and Mineral Resources (ESDM), a significant earthquake with a magnitude of 6.8 Mw occurred in Nusa Dua, Bali, on November 13, 2011, followed by at least 11 aftershocks. Some of these events were felt at an intensity of II MMI, while others were only recorded instrumentally. This seismic activity indicates ongoing tectonic stress accumulation and release, which may be associated with the identified fault structures.

Overall, the results demonstrate that the integration of GPR and electrical resistivity methods is highly effective for detecting and characterizing shallow subsurface fault systems. The presence of multiple fault structures across the study area highlights the importance of geophysical investigations in assessing geological hazards, particularly in rapidly developing regions such as Badung Regency.

4. Conclusion

The results from five survey locations consistently indicate the presence of fault structures, characterized by resistivity anomalies, disrupted stratigraphic continuity, and non-hyperbolic reflection patterns in radargrams. These features are interpreted as fault zones associated with clay-rich materials and fractured subsurface layers. The identified fault structures exhibit varying kinematic types, including both normal and reverse faults, suggesting a complex tectonic regime influenced by local and regional geological processes. The spatial distribution and characteristics of these faults are consistent with the tectonic setting of Bali, which is controlled by the subduction of the Indo-Australian Plate beneath the Eurasian Plate. This tectonic interaction generates compressional forces, volcanic activity, and structural deformation, which contribute to the development of fault systems in the study area. Additionally, local geological conditions, such as lithological heterogeneity and volcanic deposits, may further influence fault formation and reactivation. The findings have important implications for geohazard assessment, particularly in rapidly developing areas such as Badung Regency. The presence of shallow fault structures may affect ground stability, infrastructure development, and groundwater flow systems. Furthermore, the recorded seismic activity in the region supports the interpretation of ongoing tectonic processes. Overall, this study highlights the importance of integrated geophysical investigations in improving the understanding of shallow subsurface structures. The methodology and results presented here contribute to the advancement of near-surface geophysical applications and provide a valuable reference for future studies related to fault detection and hazard mitigation in tectonically active regions.

CRediT authorship contribution statement

Muhammad Amri Aziz Hakim: Writing – review & editing, Writing – original draft, Supervision, Software, Resources, Methodology, Investigation, Formal analysis, Data curation. **Shreeniwas Omanwar:** Writing – review & editing, Investigation.

Declaration of Competing Interest

The authors declare that they have no known competing financial interests or personal relationships that could have appeared to influence the work reported in this paper.

Data availability

Data will be made available on request.

Acknowledgment

The authors would like to express their sincere gratitude to all parties who contributed to the successful completion of this study. Special thanks are extended to the field survey team for their valuable assistance during data acquisition and to the local authorities in Badung Regency, particularly in Jimbaran, Pelaga, Mengwi, and Ungasan, for their support and permission to conduct this research.

References

1. Hosono, T., Hartmann, J., Louvat, P., Amann, T., Washington, K. E., West, A. J., Okamura, K., Böttcher, M. E., and Gaillardet, J. (2018). Earthquake-Induced Structural Deformations Enhance Long-Term Solute Fluxes from Active Volcanic Systems, *Scientific Reports*, Vol. 8, No. 1, 1–12. doi:10.1038/s41598-018-32735-1.
2. Zhang, Z., Yao, H., Wang, W., and Liu, C. (2021). 3-D Crustal Azimuthal Anisotropy Reveals Multi-Stage Deformation Processes of the Sichuan Basin and Its Adjacent Journal of Geophysical Research : Solid Earth, *Journal of Geophysical Research: Solid Earth*, Vol. 127, No. e2021JB023289, 1–17. doi:10.1029/2021JB023289.
3. Liu, S., Suardi, I., Xu, X., Yang, S., and Tong, P. (2021). The Geometry of the Subducted Slab Beneath Sumatra Revealed by Regional and Teleseismic Traveltime Tomography, *Journal of Geophysical Research: Solid Earth*, Vol. 126, No. 1, 1–29. doi:10.1029/2020JB020169.
4. Dewi, K. C. S., Siregar, R. N., Ningati, T. I., Pulungan, Z. N., Indriyawati, A., and Takahashi, H. (2025). Analysis of Subsurface Faults Using 3D Gravity Method Based On Satellite Image Data : Insights into Indo-Australian and Eurasian Plate Subduction in the Formation of An Accretionary Prism, *International Journal of Hydrological and Environmental for Sustainability*, Vol. 4, No. 3, 135–148. doi: 10.58524/ijhes.v4i3.960.
5. Hariyono, E., and S, L. (2018). The Characteristics of Volcanic Eruption in Indonesia, *Volcanoes - Geological and Geophysical Setting, Theoretical Aspects and Numerical Modeling, Applications to Industry and Their Impact on the Human Health*, No. July. doi:10.5772/intechopen.71449.
6. McCaffrey, R. (2009). The Tectonic Framework of the Sumatran Subduction Zone, *Annual Review of Earth and Planetary Sciences*, Vol. 37, 345–366. doi:10.1146/annurev.earth.031208.100212.
7. Hristov, V., Stoyanov, N., Valtchev, S., Kolev, S., and Benderev, A. (2019). Utilization of Low Enthalpy Geothermal Energy in Bulgaria, *IOP Conference Series: Earth and Environmental Science*, Vol. 249, No. 1. doi:10.1088/1755-1315/249/1/012035.
8. Taruna, R. M., and Banyunegoro, V. H. (2018). Earthquake Relocation Using Double Difference Method for 2D Modelling of Subducting Slab and Back Arc Thrust in West Nusa Tenggara, *Jurnal Penelitian Fisika Dan Aplikasinya (JPFA)*, Vol. 8, No. 2, 132. doi:10.26740/jpfa.v8n2.p132-143.
9. Collings, R., Lange, D., Rietbrock, A., Tilmann, F., Natawidjaja, D., Suwargadi, B., Miller, M., and Saul, J. (2012). Structure and Seismogenic Properties of the Mentawai Segment of the Sumatra Subduction Zone Revealed by Local Earthquake Traveltime Tomography, *Journal of Geophysical Research*, Vol. 117, 1–23. doi:10.1029/2011JB008469.
10. Jihad, A., Muksin, U., Syamsidik, and Ramli, M. (2021). Earthquake Relocation to Understand the Megathrust Segments along the Sumatran Subduction Zone, *IOP Conference Series: Earth and Environmental Science*, Vol. 630, 012002. doi:10.1088/1755-1315/630/1/012002.
11. Xu, J., and Kono, Y. (2002). Geometry of Slab, Intraslab Stress Field and Its Tectonic Implication in the Nankai Trough, Japan, *Earth, Planets and Space*, Vol. 54, No. 7, 733–742. doi:10.1186/BF03351726.
12. Kusuhara, F., Kazahaya, K., Morikawa, N., Yasuhara, M., Tanaka, H., Takahashi, M., and Tosaki, Y. (2020). Original Composition and Formation Process of Slab-Derived Deep Brine from Kashio Mineral Spring in Central Japan, *Earth, Planets and Space*, Vol. 72, No. 1. doi:10.1186/s40623-020-01225-y.
13. Malod, J. A., Karta, K., Beslier, M. O., and Zen, M. T. (1995). From Normal to Oblique Subduction: Tectonic Relationships between Java and Sumatra, *Journal of Southeast Asian Earth Sciences*, Vol. 12, Nos. 1–2, 85–93. doi:10.1016/0743-9547(95)00023-2.
14. Li, C. F. (2011). An Integrated Geodynamic Model of the Nankai Subduction Zone and Neighboring Regions from Geophysical Inversion and Modeling, *Journal of Geodynamics*, Vol. 51, No. 1, 64–80. doi:10.1016/j.jog.2010.08.003.
15. Stern, R. J. (2002). Subduction Zones, *Reviews of Geophysics*, Vol. 40, No. 4, 3-1-3–38. doi:10.1029/2001RG000108.
16. Utama, H. W., Mulyasari, R., and Said, Y. M. (2021). Geothermal Potential on Sumatra Fault System To Sustainable Geotourism in West Sumatra, *JGE (Jurnal Geofisika Eksplorasi)*, Vol. 7, No. 2, 126–137. doi:10.23960/jge.v7i2.128.
17. Tabei, T., Hashimoto, M., Miyazaki, S., Hirahara, K., Kimata, F., Matsushima, T., Tanaka, T., Eguchi, Y., Takaya, T., Hoso, Y., Ohya, F., and Kato, T. (2002). Subsurface Structure and Faulting of the Median Tectonic Line, Southwest Japan Inferred from GPS Velocity Field, *Earth, Planets and Space*, Vol. 54, No. 11, 1065–1070. doi:10.1186/BF03353303.
18. Tongkul, F. (2017). Active Tectonics in Sabah – Seismicity and Active Faults, *Bulletin of the Geological Society of Malaysia*, Vol. 64, No. December, 27–36. doi:10.7186/bgsm64201703.
19. Maryanto, S. (2017). Geo Techno Park Potential at Arjuno-Welirang Volcano Hosted Geothermal Area, Batu, East Java, Indonesia (Multi Geophysical Approach), *AIP Conference Proceedings*, Vol. 1908, No. 2017. doi:10.1063/1.5012712.
20. Sujitapan, C., Kendall, J. M., Chambers, J. E., and Yordkayhun, S. (2024). Landslide Assessment through Integrated Geoelectrical and Seismic Methods: A Case Study in Thungsong Site, Southern Thailand, *Heliyon*, Vol. 10, No. 2. doi:10.1016/j.heliyon.2024.e24660.
21. Chambers, J., Holmes, J., Whiteley, J., Boyd, J., Meldrum, P., Wilkinson, P., Kuras, O., Swift, R., Harrison, H., Glendinning, S., Stirling, R., Huntley, D., Slater, N., and Donohue, S. (2022). Long-Term Geoelectrical Monitoring of Landslides in Natural and Engineered Slopes, *Leading Edge*, Vol. 41, No. 11, 768–767. doi:10.1190/tle41110768.1.
22. Whiteley, J. S., Watlet, A., Uhlemann, S., Wilkinson, P., Boyd, J. P., Jordan, C., Kendall, J. M., and Chambers, J. E. (2021). Rapid Characterisation of Landslide Heterogeneity Using Unsupervised Classification of Electrical Resistivity and Seismic Refraction Surveys, *Engineering Geology*, Vol. 290, No. May, 106189. doi:10.1016/j.enggeo.2021.106189.
23. Martinho, E. (2023). *Electrical Resistivity and Induced Polarization Methods for Environmental Investigations: An Overview*, *Water, Air, and Soil Pollution* (Vol. 234), Springer International Publishing. doi:10.1007/s11270-023-06214-x.
24. Kusumayudha, S. B., Lestari, P., and Paripurno, E. T. (2018). Eruption Characteristic of the Sleeping Volcano, Sinabung, North Sumatera, Indonesia, and SMS Gateway for Disaster Early Warning System, *Indonesian Journal of Geography*, Vol. 50, No. 1, 70–77. doi:10.22146/ijg.17574.
25. Meju, M. A., and Le, L. (2002). Geoelectromagneticexploration For Natural Resources:Models, Case Studies and Challenges, *Surveys in Geophysics*, Vol. 23, 133–205.
26. Lange, D., Tilmann, F., Henstock, T., Rietbrock, A., Natawidjaja, D., and Kopp, H. (2018). Structure of the Central Sumatran Subduction Zone Revealed by Local Earthquake Travel-Time Tomography Using an Amphibious Network, *Solid Earth*, Vol. 9, No. 4, 1035–1049. doi:10.5194/se-9-1035-2018.
27. Lin, J. Y., Sibuet, J. C., Hsu, S. K., and Wu, W. N. (2014). Could a Sumatra-like Megathrust Earthquake Occur in the South Ryukyu Subduction Zone?, *Earth, Planets and Space*, Vol. 66, No. 1, 1–8. doi:10.1186/1880-5981-66-49.
28. Siringoringo, L. P., Sapiie, B., Rudyawan, A., and Sucipta, I. G. B. E. (2024). Origin of High Heat Flow in the Back-Arc Basins of Sumatra: An Opportunity for Geothermal Energy Development, *Energy Geoscience*, Vol. 5, No. 3, 100289. doi:10.1016/j.engeos.2024.100289.
29. Hochstein, M. P., and Sudarman, S. (1993). Geothermal Resources of Sumatra, *Geothermics*, Vol. 22, No. 3, 181–200. doi:10.1016/0375-6505(93)90042-L.